ELSEVIER

Biochimica et Biophysica Acta 1461 (1999) 58–68

BIOCHIMICA ET BIOPHYSICA ACTA
BBA

www.elsevier.com/locate/bba

Location and orientation of DODCI in lipid bilayer membranes: effects of lipid chain length and unsaturation

M.M.G. Krishna, N. Periasamy *

Department of Chemical Sciences, Tata Institute of Fundamental Research, Homi Bhabha Road, Colaba, Mumbai 400 005, India

Received 6 July 1999; received in revised form 18 August 1999; accepted 25 August 1999

Abstract

The location and orientation of a linear dye molecule, DODCI, in lipid bilayer membrane were determined by the effect of viscosity and refractive index of the aqueous medium on the fluorescence properties of the dye bound to the membrane. The membrane-bound dye is solubilized in two sites, one near the surface (short fluorescence lifetime) and another in the interior of the membrane (long lifetime). The ratio of the dye in the two locations and the orientation of the dye (parallel or perpendicular to the membrane) are sensitive to the lipid chain length and unsaturation in the alkyl chain. The fraction of the dye in the interior region is higher for short alkyl chains (C12 > C14 > C16 ≫ C18 ≈ C20) and in unsaturated lipids (C14:1 > C14:0, C16:1 > C16:0). These experimental results are consistent with the general principle that the penetration of an amphiphilic organic molecule into the interior region of the membrane is more when the structure of the bilayer is more fluid-like.

Keywords: Membrane; 3,3′-Diethyloxadicarbocyanine iodide; Location; Orientation; Chain length; Unsaturation

1. Introduction

Small molecules are often used to probe biological environments. The use of spin labels and fluorescent probes are some of the well-known examples of the use of small molecules in the study of biological systems. To understand the mechanisms of different processes involving the small molecules and/or to make use of these small molecules in the study of biological systems, one needs to know the location and orientation of these molecules in the biological systems. The location, orientation and dynamics of small molecules in lipid bilayer membranes and the way the lipid molecules modify the structure and dynamics have been the subject of many studies.

Fluorescent probe molecules are commonly employed to understand the structure and dynamics of biological membranes in relation to membrane related functions [1–6]. Most of these molecules are lipophilic in nature and are preferentially solubilized in lipid bilayer membranes. The location and orientation of these small molecules in a lipid bilayer membrane have been the subject of numerous studies [1,4,5,7–26]. A novel method used recently is the effect of refractive index and viscosity of the aqueous medium on the fluorescence lifetime of the membrane-bound fluorophore which can reveal the location of the fluorophore in the membrane [27] and the orientational distribution [28]. Here we address the

* Corresponding author. Fax: +91 (22) 2152110/2181; E-mail: peri@tifr.res.in

0005-2736/99/$ – see front matter
PII: S0005-2736(99)00149-2

effect of lipid parameters on the location and orientation of linear molecules in a lipid bilayer membrane with the help of the effect of aqueous phase parameters on the fluorescence lifetime of the membrane-bound fluorescent molecule.

The aqueous phase parameters such as viscosity and refractive index affect the fluorescence properties of the membrane-bound dye [20,22,27–29]. Increasing viscosity increases the fluorescence lifetime by decreasing the non-radiative rate whereas increasing the refractive index decreases the lifetime by increasing the radiative rate. Hence, viscosity and refractive index have opposite effects on the fluorescence lifetime of a membrane-bound dye. Viscosity effect is based on the collisional mechanism and hence this is the predominant effect for the dye molecules located near the surface of the membrane which are exposed to the aqueous phase. Refractive index effect is purely optical and is dominant for the probes located in the core/interior region of the bilayer. These two effects were used to determine the location and orientation of linear molecules in lipid bilayer membranes [27,28]. It has been shown that the dicarbocyanines such as DODCI, cationic dye, is partitioned between aqueous and membrane phase and the fluorescence spectra and lifetimes in the two phases can be separated by a new method called spectrally constrained global analysis [29]. It was shown that the membrane-bound dye exists in two different locations, one at the surface/interface and the other in the core/interior region of the bilayer [27]. The dye in the core/interior region exists in two different orientations, one parallel to the lipid chains and the other parallel to the membrane surface [28]. In this paper, we report how the lipid parameters such as the lipid chain length and unsaturation affect the distribution of DODCI between surface and interior regions of the bilayer, and the change in the ratio of the two different orientations in the interior region of the bilayer.

2. Materials and methods

Fluorescence measurements were carried out on DODCI (3,3′-diethyloxadicarbocyanine iodide; Exciton, USA) incorporated in the vesicles made up of different lipids C12:0 (DLPC, dilauroylphosphatidylcholine), C14:0 (DMPC, dimyristoyl PC), C16:0 (DPPC, dipalmitoyl PC), C18:0 (DSPC, distearoyl PC), C20:0 (DAPC, diarachidoyl PC), C14:1 (dimyristoleyl PC) and C16:1 (dipalmitoleyl PC). The nomenclature used here in representing a phosphatidylcholine (PC) lipid is as follows. The lipid is represented as Cx:y where x represents the length of the alkyl chain and y represents the number of double bonds in the alkyl chain. The single double bond in the alkyl chain of some of the lipids (C14:1 and C16:1) is at the 9th position and is of *cis* type. The lipids were purchased from Avanti Polar Lipids (USA). Fig. 1 shows the structure of the dye DODCI. The single exponential fluorescence lifetime of DODCI in ethanol is 1.07 ns. Fluorescence experiments were carried out on the dye incorporated in sonicated vesicles prepared in seven aqueous sucrose solutions ranging from 0% to 44.4% w/w. The sonicated liposomes were prepared in pH 4.3 buffer (10 mM CH_3COONa, 10 mM NaH_2PO_4, 10 mM MES (2-[*N*-morpholino]ethanesulfonic acid) and 150 mM NaCl) as described in [30]. Here sucrose is used to vary the viscosity and refractive index of the aqueous medium. Increasing the sucrose concentration from 0% to 44.4% (w/w) increased the refractive index from 1.334 to 1.413. At the same time, the relative viscosity of the aqueous solution increases from 1 to 10.74. The lipid concentration used in these experiments was about 0.1 mg/ml (0.14 mM). The dyes were added from the stock solution made in ethanol to the vesicles and kept overnight. The final samples contained less than 1% v/v ethanol. The dye to lipid ratio was kept at approx. 1:500.

The steady state fluorescence intensity and anisotropy measurements were made using either a Shimadzu RF540 or a SPEX Fluorolog 1681 T format

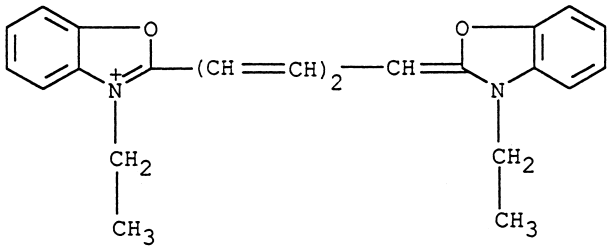

DODCI

Fig. 1. Structure of DODCI.

spectrofluorophotometer. The time resolved fluorescence measurements were made using a high repetition rate (800 kHz) picosecond dye laser (rhodamine 6G) coupled with time correlated single photon counting (TCSPC) setup described elsewhere [31,32], currently using a microchannel plate photomultiplier (Hamamatsu 2809). The time resolved fluorescence intensity and anisotropy measurements were made at long wavelengths of excitation (580 nm) and emission (690 nm) to avoid the contribution from the dye present in water as described before [27,29]. The sample was excited with vertically polarized light and the fluorescence decay was collected with emission polarizer kept at magic angle ($\approx$54.7°) with respect to the excitation polarizer for measuring lifetimes. For the anisotropy measurements, the fluorescence intensity decays were measured with the emission polarizer set at parallel or perpendicular orientation with respect to the excitation polarizer. Geometry factor (G-factor) for the TCSPC setup was determined by the tail matching method using DODCI in ethanol for which the rotational correlation time (0.25 ns) is much faster than its fluorescence lifetime (1.07 ns). The instrument response function (IRF) was recorded using a non-dairy creamer scattering solution. The full width at half-maximum (FWHM) of IRF is about 200 ps. Typical peak count in the emission decay for fluorescence intensity and anisotropy measurements was about 10 000. Time per channel was 37.84 ps.

The experimentally measured fluorescence decay data, $F(t)$, are a convolution of the instrument response function, $R(t)$, with the intensity decay function, $I(t)$:

$$F(t) = \int_0^t R(s+\delta)\, I(t-s)\mathrm{d}s \tag{1}$$

where δ is the shift parameter. In discrete exponential analysis, the intensity decay function is represented as a normalized multi-exponential as

$$I(t) = \sum_i \alpha_i \exp(-t/\tau_i) \tag{2}$$

where α_i and τ_i are the amplitudes and the lifetimes with $\Sigma_i \alpha_i = 1$. The parameters of the decay function $I(t)$, namely, α_i and τ_i were determined using experimentally determined $F(t)$ and $R(t)$ by iterative deconvolution procedure using Levenberg-Marquardt algorithm for optimization of the parameters [31,33,34]. The goodness of fit of experimental $F(t)$ and calculated $F(t)$ is judged by the χ^2 value (close to 1) and the random residual distribution. The precision of the values of the lifetimes and amplitudes was improved by global analysis of at least six fluorescence decays for each sample, each decay having 10 000 counts at the peak [31,35].

The time resolved anisotropy decay $r(t)$ was calculated using the parallel ($I_\parallel(t)$) and perpendicular polarized ($I_\perp(t)$) intensity decays as

$$r(t) = \frac{I_\parallel - GI_\perp}{I_\parallel + 2GI_\perp} \tag{3}$$

where G is the G-factor for the TCSPC setup. The polarized intensity decays $I_\parallel(t)$ and $I_\perp(t)$ were obtained by deconvolution procedure from the experimentally measured polarized fluorescence decays $F_\parallel(t)$ and $F_\perp(t)$ with the instrument response function $R(t)$.

2.1. Determination of order parameters

2.1.1. Order parameter from fluorescence lifetime measurements

The radiative rate of a linear fluorescent molecule in bilayer membrane is given by [20,36]

$$k_\mathrm{r} = \frac{4\omega^3}{3\hbar c^3} f^2 |\mu|^2 n_0 \left(\sin^2\theta + \frac{n_0^4}{n_1^4}\cos^2\theta\right) \tag{4}$$

where ω is the circular frequency of fluorescence light, $\hbar$ is the Planck's constant, c is the speed of light, f is a factor which accounts for the difference between the local electric field experienced by the dye and the macroscopic field inside the layer, μ is the matrix element of the emission electric dipole operator, n_0 and n_1 are the refractive indices of the aqueous medium and the bilayer, and θ is the angle between the molecular emission dipole and the normal to the surface of the bilayer. This equation is based on an isotropic refractive index (n_1) for the bilayer membrane. The effect of anisotropy in the index of refraction (birefringence) of the bilayer, if any, is assumed to be negligible. If k_nr is the non-radiative rate (experimentally determined) then fluorescence lifetime is $(k_\mathrm{r}+k_\mathrm{nr})^{-1}$. The fluorescence decay of the molecule is faster (lifetime decreases as a result

of the increase in the radiative rate) with the increase in the refractive index of the aqueous solution which is experimentally observed for a few linear molecules such as DODCI [20,27–29]. If $P(\theta)$ is the orientational distribution of the linear molecules with respect to the membrane normal, the second rank order parameter $\langle P_2(\cos\theta)\rangle_\tau$ can be determined from the variation of k_r ($=\tau^{-1}-k_{nr}$) with n_0 and from Eq. 4 [20] as

$$\langle P_2(\cos\theta)\rangle_\tau = \frac{An_1^4 - \frac{1}{2}B}{An_1^4 + B} \quad (5)$$

where A and B are the slope and intercept of the linear plot

$$\frac{(\frac{1}{\tau} - k_{nr})}{n_0} = An_0^4 + B \quad (6)$$

The subscript τ indicates that the order parameter is determined from the lifetime data.

The refractive index of the membrane n_1 is determined as described in [20,28]. The calculation of the order parameter $\langle P_2(\cos\theta)\rangle_\tau$ requires the estimation of k_{nr} for the particular species associated with the long lifetime. In a multicomponent membrane system, k_{nr} for one component cannot be determined. Hence, k_{nr} for the membrane-bound dye was determined as follows. The radiative rate k_r for the membrane-bound dye is independent of the orientation when the refractive indices of the membrane phase (n_1) and aqueous phases (n_0) match (see Eq. 4). Therefore, the value of k_r in the membrane was taken equal to the value of k_r determined in an aqueous glycerol solution whose refractive index matched with that of the membrane [28]. In order to minimize the errors associated with this method, the experiments on lipid systems described here were carried out at 5°C which decreases the contribution of non-radiative processes to the fluorescence lifetime.

The phase transition temperatures for the lipids used in this study are as follows: −2, 24 and 41°C for the saturated lipids C12:0, C14:0 and C16:0, respectively, and below 0°C for the unsaturated lipids C14:1 and C16:1 [37–39]. Thus, at the temperature where the experiments were carried out, i.e., at 5°C, C14:0 and C16:0 remain in the gel phase and others are in the liquid crystalline phase.

2.1.2. Order parameter from anisotropy measurements

The second rank order parameter can also be determined from the values of anisotropy at infinite time (r_∞) and at zero time (r_0) using the equation [1,40,41]

$$\langle P_2(\cos\theta)\rangle_a = \left(\frac{r_\infty}{r_0}\right)^{\frac{1}{2}} \quad (7)$$

The subscript a indicates that the order parameter is determined from the anisotropy data. This measures the orientational freedom of the probe population in the bilayer.

3. Results

3.1. Location of DODCI

The fluorescence of DODCI in lipid vesicles arises due to the dye partitioned between the aqueous phase and the membrane phase [27,29]. Fluorescence measurements were done at long excitation (580 nm) and emission wavelengths (690 nm) so that the contribution to the measured fluorescence decay from the dye component in aqueous phase is negligible [27,29]. In all the lipid bilayer vesicles made of different lipids used in this study, the membrane-bound DODCI showed two lifetimes, the short lifetime $\tau_s \approx 1.0$ ns and the long lifetime $\tau_l \approx 2.0$ ns. The values of the lifetimes in the case of different lipid systems are given in Table 1. With the variation of sucrose concentration in the aqueous phase, these two lifetimes showed different trends compared to that of the dye present in the aqueous phase. Fig. 2 shows the typical trend observed for the dye in aqueous solution and when bound to the membrane. As mentioned before, increase of sucrose increases both the viscosity and refractive index of the aqueous medium. Increase of viscosity increases the fluorescence lifetime and this effect is predominant for the dye molecules that are located near the surface of the membrane. Increase of refractive index decreases the fluorescence lifetime and this effect is observable for the dyes located in the core of the membrane. With the increase of the sucrose concentration in the aqueous phase, the τ_s component at first showed a slight decrease or no variation and then increased with the increase in sucrose concentration. The ob-

Table 1
Fluorescence decay parameters and order parameters of DODCI in bilayer membranes made up of different lipids

Lipid	τ_s (ns)	τ_l (ns)	m	$\langle P_2\rangle_\tau$	r_∞	$\langle P_2\rangle_a$
C12:0	1.01	1.87	2.9	0.510	0.23	0.778
C14:0	1.08	2.10	3.3	0.485	0.22	0.761
C16:0	1.02	1.88	3.1	0.645	0.24	0.795
C14:1	0.96	1.95	2.6	0.341	0.23	0.788
C16:1	0.99	1.96	3.1	0.605	0.26	0.833

τ_s and τ_l represent the short and long lifetimes of the membrane-bound dye. $\langle P_2\rangle_\tau$ and $\langle P_2\rangle_a$ are the two order parameters determined from fluorescence lifetime and anisotropy measurements. m value is obtained by fitting the long lifetime data to the equation $\tau_l \propto (n_0)^{-m}$ where n_0 is the refractive index of the aqueous medium in which vesicles were made. The values of anisotropy at infinite time (r_∞) determined from time resolved anisotropy decay are also shown. Anisotropy at zero time (r_0) is determined to be 0.375 from the time resolved anisotropy decay of DODCI in glycerol.

served trend is a dominant viscosity effect over the refractive index effect and is characteristic of the dye molecules located on the surface region of the membrane [27,29]. The long lifetime steadily decreases which is a refractive index effect indicating that this lifetime corresponds to that of the dye located in the interior region of the bilayer membrane [27–29]. The ratio of the amplitudes (α_i in Eq. 2) of the long and short lifetimes is equal to the ratio of population of

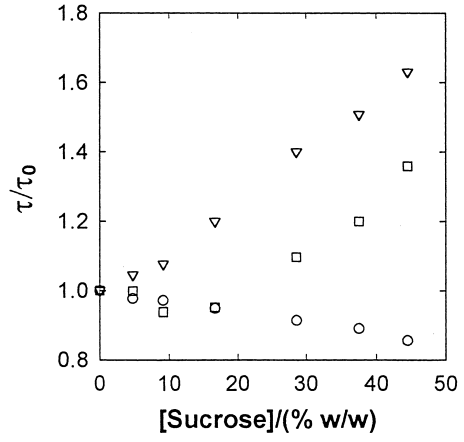

Fig. 2. Variation of the fluorescence lifetime ratio (τ/τ_0) for DODCI with the concentration of sucrose. ▽, DODCI in aqueous solution; ○, DODCI bound to the membrane (long lifetime, τ_l); □, DODCI bound to the membrane (short lifetime, τ_s).

the dye molecules in the interior and surface regions of the membrane with the assumption that the radiative rate and molar extinction coefficient at the excitation wavelength for the dye in the two locations are the same.

3.1.1. Effect of chain length

Fig. 3A and B show the variation of the amplitudes of the long and short lifetimes of the membrane bound dye with the alkyl chain length. Fig. 3A shows the case for the saturated lipids C12:0, C14:0 and C16:0 and Fig. 3B shows the case of unsaturated lipids C14:1 and C16:1. As discussed earlier, the amplitudes of the short and long lifetimes of the membrane-bound DODCI represent the populations of the dye in two different locations: surface and interior regions of the bilayer, respectively. It is clear from the figure that in both the cases of saturated and unsaturated lipids, the dye population located in the interior of the membrane decreases with the increase of the lipid chain length. That means, the dye penetrating into the membrane decreases with the increase of the chain length. This effect is so severe that in the case of lipids with longer alkyl chains such as C18:0 (DSPC) and C20:0 (DAPC), the dye penetrating into the interior of the membrane is extremely low and no long lifetime component was observed. This effect of chain length on location is found to be the same for those lipids that exist in the gel phase (C14:0 and C16:0 at 5°C) as well as for those that are in the liquid crystalline phase (C14:1 and C16:1 at 5°C).

3.1.2. Effect of unsaturation

The effect of lipid unsaturation on the amplitudes of the short and long lifetimes of membrane-bound DODCI are shown in Fig. 3C and D. Fig. 3C and D show the variation with the presence of one double bond for the lipid chain length 14 (C14:0 and C14:1) and 16 carbon atoms (C16:0 and C16:1), respectively. It is clear from the figure that the fraction of the dye located in the interior (long lifetime) of the bilayer has increased with unsaturation in the lipid chain. At 5°C, the saturated lipids C14:0 and C16:0 are in the gel phase whereas the unsaturated lipids C14:1 and C16:1 are in the liquid crystalline phase.

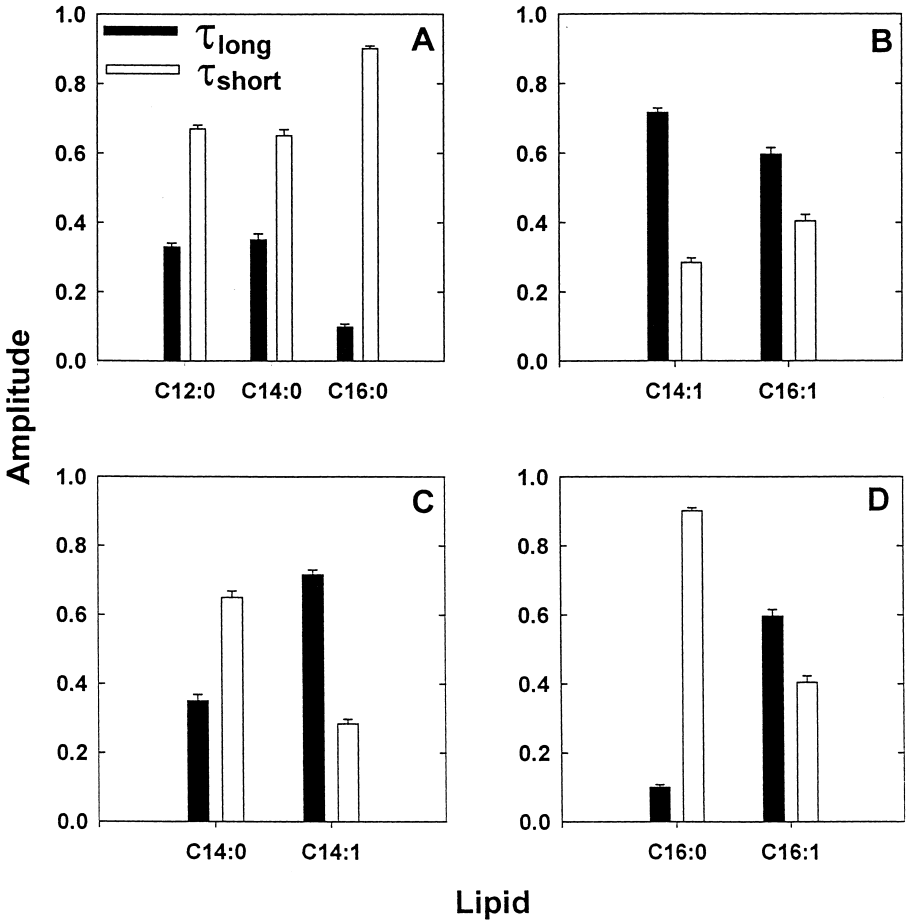

Fig. 3. Variation of the amplitudes of the long and short lifetimes of the membrane bound DODCI with the alkyl chain length and unsaturation. These two amplitudes represent the relative fraction of the dye located at two different sites: core and surface regions of the bilayer respectively. The sum of the two amplitudes is normalized to unity. A and B indicate the variation with the alkyl chain length for saturated and unsaturated lipids respectively. C and D show the variation with unsaturation for the case of C14:0 and C14:1; and C16:0 and C16:1 respectively.

3.2. Orientation of DODCI

As described in the previous section, a significant fraction of the dye (τ_{long}) is located in the interior region of the bilayer. The order parameter $\langle P_2 \rangle_\tau$ for this population was determined from the refractive index effect on the long lifetime and $\langle P_2 \rangle_a$ was determined from the time resolved anisotropy measurements, as described in Section 2. Table 1 shows the long lifetimes and the two order parameters obtained in different lipid vesicles. The two order parameters were used to obtain the bimodal orientational distribution of DODCI in different lipid bilayer membranes, according to the Brownian rotational diffusion (BRD) model [28]. In this case, the orientational distribution $P(\theta)$ is considered as a sum of two orientational populations, one centered about the membrane normal $P'(\theta)$ and the other parallel to the membrane surface $P''(\theta)$.

$$P(\theta) = P'(\theta) + P''(\theta) \tag{8}$$

where θ is the angle measured with respect to the membrane normal. $P(\theta)$ has to satisfy the normalization condition:

$$\int_0^\pi P(\theta) \sin\theta \, d\theta = 1 \tag{9}$$

$\langle P_2 \rangle_\tau$ is calculated with respect to the membrane normal as

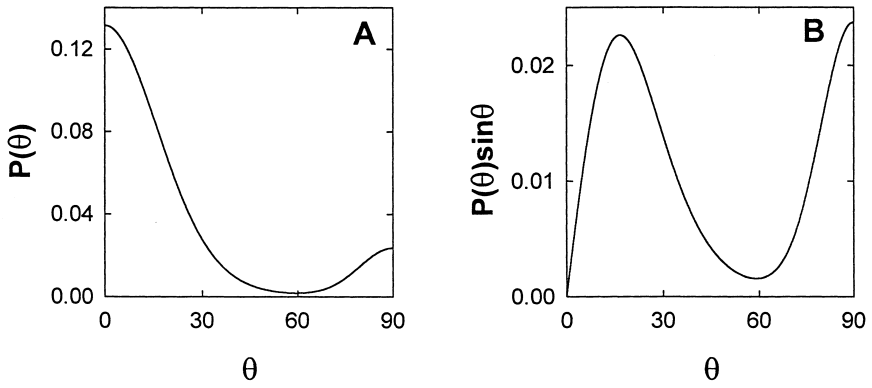

Fig. 4. (A) Bimodal orientational distribution function, $P(\theta)$, and (B) population distribution function, $P(\theta)\sin\theta$, for DODCI in C14:1.

$$\langle P_2(\cos\theta)\rangle_\tau = \int_0^\pi P_2(\cos\theta)P(\theta)\,\sin\theta\,\mathrm{d}\theta \qquad (10)$$

$\langle P_2\rangle_a$ is calculated by taking into account the fact that the director axes for the two distributions are mutually perpendicular.

$$\langle P_2(\cos\theta)\rangle_a =$$

$$\int_0^\pi [P'(\theta)P_2(\cos\theta) + P''(\theta)P_2(\cos(\pi/2-\theta))]\sin\theta\,\mathrm{d}\theta \qquad (11)$$

In the simplest case of the Maier-Saupe model [10,26], the two orientational distributions $P'(\theta)$ and $P''(\theta)$ can be written as

$$P'(\theta) = a_1\,\exp(\lambda_1 P_2(\cos\theta)),$$

$$\mathrm{P''}(\theta) = \mathrm{a_2}\,\exp(-\lambda_2 \mathrm{P_2}(\cos\theta)) \qquad (12)$$

where a_1 and a_2 are the amplitudes and λ_1 (>0) and λ_2 (>0) are the adjustable parameters consistent with the normalization condition (Eq. 9). Fig. 4A shows the orientational distribution and Fig. 4B shows the population distribution obtained in the case of DODCI in C14:1. The fractional populations f_{para} and f_{perp} were calculated from the area of the two distributions in Fig. 4B. In general, the population oriented parallel to the membrane normal (f_{para}) is higher than that oriented perpendicular to the membrane normal (f_{perp}) in the bimodal orientational distribution for all lipids. The results of fractional populations in the two orientations for all lipids are summarized in Fig. 5.

3.2.1. Effect of chain length

The variation of the fractional amplitudes in the two orthogonal orientational distributions with the chain length are shown in Fig. 5A and B. Fig. 5A shows the case for saturated lipids (C12:0, C14:0 and C16:0) and Fig. 5B shows the variation in the case of unsaturated lipids (C14:1 and C16:1). The fraction of the probe molecules oriented parallel to the lipid chain (f_{para}) increases with the increase of the chain length for both saturated and unsaturated lipids. The observed effect of chain length is the same for both the gel phase lipids (C14:0 and C16:0 at 5°C) and for the liquid crystalline phase lipids (C14:1 and C16:1 at 5°C).

3.2.2. Effect of unsaturation

Fig. 5C and D show the variation in the fractional amplitudes of the two orientational distributions with the unsaturation in the lipid chain. These two figures show the variation with the presence of one double bond for the case where the lipid chain length is kept constant at 14 (C14:0 and C14:1) and 16 carbon atoms (C16:0 and C16:1), respectively. The probe molecules that are oriented parallel to the membrane normal decrease with the introduction of a double bond in the lipid chain.

4. Discussion

The solubilization of organic molecules and the location and orientation of organic molecules in the bilayer membrane have been the subject of numerous

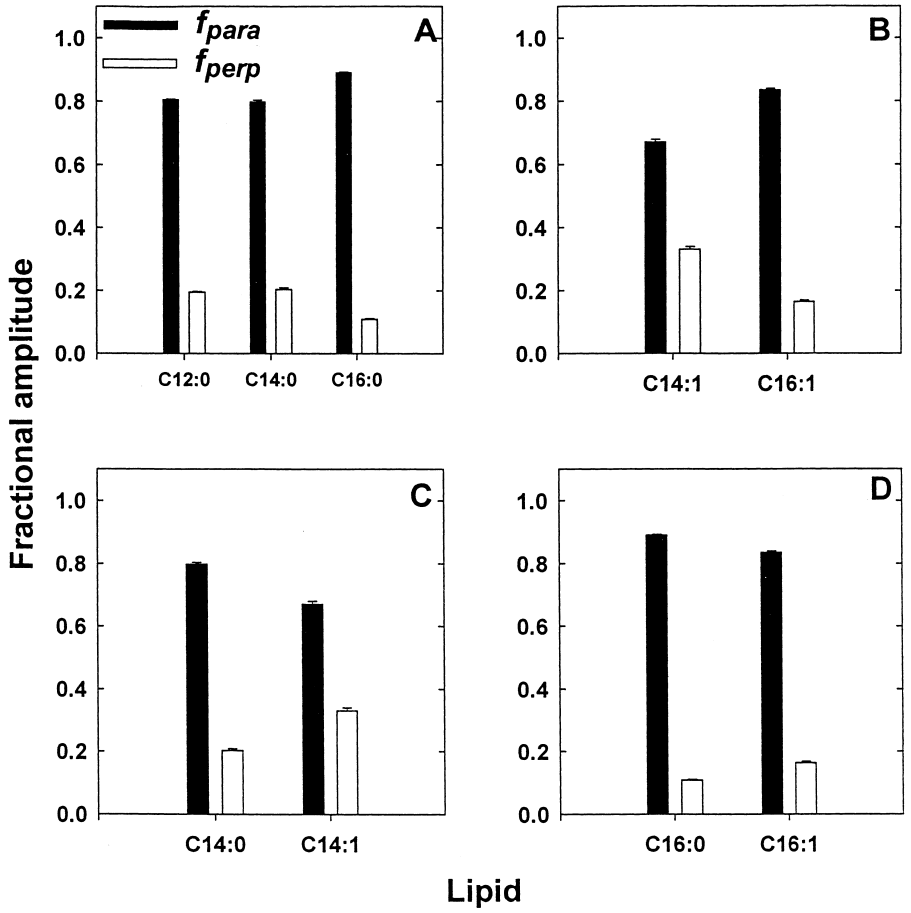

Fig. 5. Variation of the fractional amplitudes in the two orthogonal orientational distributions of the bimodal orientational distribution with the chain length and unsaturation. f_{para} and f_{perp} represent the population of the probe molecules oriented in the two distributions with the respective director axes parallel and perpendicular to the bilayer membrane normal. The sum of these were normalized to unity. A and B indicate the variation with lipid chain length in the case of saturated lipids C12:0, C14:0 and C16:0, and in the case of unsaturated lipids C14:1 and C16:1 respectively. C and D show the variation with unsaturation in the case of C14:0 and C14:1, and C16:0 and C16:1 respectively.

studies. In recent years, molecular dynamics simulations have given a better understanding of the structure of the bilayer and variation of physical properties (microviscosity, polarity, etc.) in different regions of the bilayer [42]. Based on several studies, a four region model for the bilayer membrane has been proposed [42]. Region 1 is the aqueous side of the bilayer called the region of 'perturbed water'. Considerable mobility of lipid molecules in a direction perpendicular to the surface is indicated in this region. Region 2 is the interphase region that contains all of the head group atoms and some of the tail atoms. The density is maximum in this region and the free volume is minimum in this part of the bilayer. Region 3 is called 'soft polymer' region consisting of partially ordered chains resembling a soft polymer in density and properties. This region has a high tail density and low free volume. Region 4 is the decane-like hydrocarbon region characterized by a low density and high fraction of free volume compared to other regions. The location of organic molecules in different regions will depend on the structure of the lipid, structure of the organic dye molecule and the free volume available for it in different regions of the bilayer. DODCI, being linear and cationic, we attribute the location of the dye present in the interior of the membrane, somewhere in between region 3 and region 4 of the proposed bilayer structure and hence most of the observed orientational distributions have a maximum popula-

tion towards the parallel orientation along the membrane normal compared to the perpendicular orientation. More neutral molecules may penetrate deeper into the bilayer (completely into region 4) where the available free volume is large.

For the lipids that were used in this study the head group was the same and hence regions 1 and 2 are likely to be similar. The variation of alkyl chain length and unsaturation affect the physical characteristics of regions 3 and 4. Phase transition temperature is clearly a manifestation of the lipid organization in these regions. At the temperature at which experiments were done (5°C), the lipids C14:0 and C16:0 exist in the gel phase whereas the other lipids C12:0, C14:1 and C16:1 are in the liquid crystalline phase. The results on the location and orientation of DODCI in the lipids of varying chain length show that increase of chain length decreases the amount of dye penetrating into the interior of the bilayer and in the interior of the bilayer, it increases the population of the dye molecules oriented parallel to the membrane normal compared to the perpendicular orientation. This is found to be true when the comparison is done among lipids that exist in the gel phase (C14:0 and C16:0), or among the lipids that exist in the liquid crystalline phase (C14:1 and C16:1). This indicates that the density of the lipid chains increases at the interior of the membrane with the increase of the chain length. This is evident from some of the experimental and simulation studies carried out on lipids of varying chain lengths which show that the interaction between the lipid chains of the two leaves of the bilayer is less for the membranes made up of shorter alkyl chain lengths compared to that of longer alkyl chain lengths [38,43,44].

Comparison of the results between the saturated and unsaturated lipids (with one double bond) with the same alkyl chain length shows that the increase of unsaturation increases the penetration of the dye into the interior of the bilayer and the population of the parallel orientation with the membrane surface increases in the interior of the bilayer. At 5°C, the two saturated lipids C14:0 and C16:0 are in the gel phase whereas the two unsaturated lipids C14:1 and C16:1 are in the liquid crystalline phase. The presence of the *cis* double bond at the ninth position in the lipid chain results in the lower packing density of the unsaturated lipids compared to the saturated lipids, which is also responsible for the observed phase change from gel to liquid crystalline phase with unsaturation in these lipids. The penetration of the small molecules into the lipid bilayer is higher in the case of liquid crystalline bilayers compared to the gel phase bilayers [42,44,45]. Increased hydration levels of the bilayer with the increase of unsaturation in the lipid chain may also be due to lower packing density [15,46,47]. The increased area per head group in the liquid crystalline phase allows for more mobility of the hydrocarbon tails that reduces the tight packing of the lipid chains compared to the gel phase [42,44,45]. It is also observed that the mobility of the double bonded lipid chains is much higher, particularly at the position of the unsaturation compared to the saturated lipid chains [42,44,45]. In the case of unsaturated lipid chains, the average angle of the *cis* double bond with respect to the membrane normal is found to be close to 40° [42,44,45]. Because of these factors, the free volume available in the interior of the membrane is less for the parallel orientation of the dye molecules in unsaturated lipids compared to the saturated lipids of the same chain length.

In summary, we have used the fluorescent probe DODCI in different lipid bilayer membranes to understand how the location and orientation of linear molecules in bilayer membranes are affected by the lipid parameters such as alkyl chain length and unsaturation. The order parameter $\langle P_2 \rangle_\tau$ and the relative populations in the two orientations in the bimodal orientational distribution, f_{para} and f_{perp} are the new parameters used in characterizing the orientational distribution of linear dye molecules in lipid bilayer membranes in addition to the conventional order parameter $\langle P_2 \rangle_a$. In the membranes made up of lipids with short alkyl chain length or with unsaturated alkyl chains, DODCI is preferentially located in the interior region of the bilayer compared to the surface. Short alkyl chain and unsaturation in the lipid chain increase the fractional population that is oriented perpendicular to the membrane normal.

Acknowledgements

The authors thank Prof. A.S. Verkman of the University of California, San Francisco for partial sup-

port of this work through NIH Fogarty Research Award TW 00704.

References

[1] J.R. Lakowicz, Principles of Fluorescence Spectroscopy, Plenum Press, New York, 1983.
[2] C.D. Stubbs, B.W. Williams, Fluorescence in membranes, in: J.R. Lakowicz (Ed.), Topics in Fluorescence Spectroscopy, vol. 3, Plenum Press, New York, 1992.
[3] T.G. Dewey (Ed.), Biophysical and Biochemical Aspects of Fluorescence Spectroscopy, Plenum Press, New York, 1991.
[4] B.R. Lentz, Membrane fluidity as detected by diphenylhexatriene probes, Chem. Phys. Lipids 50 (1989) 171–190.
[5] B.R. Lentz, Use of fluorescent probes to monitor molecular order and motion within liposome bilayers, Chem. Phys. Lipids 64 (1993) 99–116.
[6] R.P. Haugland, Handbook of Fluorescent Probes and Research Chemicals, 6th edn., Molecular Probes Inc., 1996.
[7] R.A. Badley, W.G. Martin, H. Schneider, Dynamic behaviour of fluorescent probes in lipid bilayer membranes, Biochemistry 12 (1973) 268–275.
[8] K. Kinosita Jr., S. Kawato, A. Ikegami, A theory of fluorescence polarization decay in membranes, Biophys. J. 20 (1977) 289–305.
[9] G. Lipari, A. Szabo, Effect of librational motion on fluorescence depolarization and nuclear magnetic resonance relaxation in macromolecules and membranes, Biophys. J. 30 (1980) 489–506.
[10] C. Zannoni, A. Aricioni, P. Cavatorta, Fluorescence depolarization in liquid crystals and membrane bilayers, Chem. Phys. Lipids 32 (1983) 179–250.
[11] A. Szabo, Theory of fluorescence depolarization in macromolecules and membranes, J. Chem. Phys. 81 (1984) 150–167.
[12] W. van der Meer, H. Pottel, W. Herrman, M. Ameloot, H. Hendrickx, H. Schroder, Effect of orientational order on the decay of the fluorescence anisotropy in membrane suspensions. A new approximate solution of rotational diffusion equation, Biophys. J. 46 (1984) 515–523.
[13] M. Ameloot, H. Hendrickx, W. Herreman, H. Pottel, F.V. Cauvelaert, W. van der Meer, Effect of orientational order on the decay of the fluorescence anisotropy in membrane suspensions: experimental verification on unilamellar vesicles and lipid/α-lactalbumin complexes, Biophys. J. 46 (1984) 525–539.
[14] A. Chattopadhyay, E. London, Parallax method for direct measurement of membrane penetration depth utilizing fluorescence quenching by spin-labeled phospholipids, Biochemistry 26 (1987) 39–45.
[15] M. Straume, B. Litman, Equilibrium and dynamic structure of large, unilamellar, unsaturated acyl chain phosphatidylcholine vesicles. Higher order analysis of 1,6-diphenyl-1,3,5-hexatriene and 1-[4-(trimethylammonio)phenyl]-6-phenyl-1,3,5-hexatriene anisotropy decay, Biochemistry 26 (1987) 5113–5120.
[16] M. Straume, B. Litman, Influence of cholesterol on equilibrium and dynamic bilayer structure of unsaturated acyl chain phosphatidylcholine vesicles as determined from higher order analysis of fluorescence anisotropy decay, Biochemistry 26 (1987) 5121–5126.
[17] J.C. Smith, Potential-sensitive molecular probes in membranes of bioenergetic relevance, Biochim. Biophys. Acta 1016 (1990) 1–28.
[18] S. Wang, J.M. Beechem, E. Gratton, M. Glaser, Orientational distribution of 1,6-diphenyl-1,3,5-hexatriene in phospholipid vesicles as determined by global analysis of frequency domain fluorimetry data, Biochemistry 30 (1991) 5565–5572.
[19] D.A. van der Sijis, E.E. van Faasen, Y.K. Levine, The interpretation of fluorescence anisotropy decays of probe molecules in membrane systems, Chem. Phys. Lett. 216 (1993) 559–565.
[20] D. Toptygin, L. Brand, Fluorescence decay of DPH in lipid membranes: influence of the external refractive index, Biophys. Chem. 48 (1993) 205–220.
[21] J.M. Muller, E.E. van Faassen, G. van Ginkel, Experimental support for a novel compound motion model for the time-resolved fluorescence anisotropy decay of TMA-DPH in lipid vesicle bilayer, Chem. Phys. 185 (1994) 393–404.
[22] D. Toptygin, L. Brand, Determination of DPH order parameters in unoriented vesicles, J. Fluoresc. 5 (1995) 39–50.
[23] U.A. van der Heide, G. van Ginkel, Y.K. Levine, DPH is localised in two distinct populations in lipid vesicles, Chem. Phys. Lett. 253 (1996) 118–122.
[24] A.S. Holmes, D.J.S. Birch, A. Sanderson, G.G. Aloisi, Time-resolved fluorescence photophysics of trans-stilbene in a DPPC lipid bilayer: evidence for a free rotation, location within two sites and a pre-liquid crystalline phase transition, Chem. Phys. Lett. 266 (1997) 309–316.
[25] M.A.M.J. van Zandvoort, H.C. Gerritsen, Y.K. Levine, Distribution of hydrophobic probe molecules in lipid bilayers. 1. Monte Carlo dynamics computer simulations, J. Phys. Chem. B 101 (1997) 4142–4148.
[26] M.A.M.J. van Zandvoort, H.C. Gerritsen, G. van Ginkel, Y.K. Levine, R. Tarroni, C. Zannoni, Distribution of hydrophobic probe molecules in lipid bilayers. 2. Time-resolved fluorescence anisotropy study of perylene in vesicles, J. Phys. Chem. B 101 (1997) 4149–4154.
[27] M.M.G. Krishna, N. Periasamy, Fluorescence of organic dyes in lipid membranes: site of solubilization and effects of viscosity and refractive index on lifetimes, J. Fluoresc. 8 (1998) 81–91.
[28] M.M.G. Krishna, N. Periasamy, Orientational distribution of linear dye molecules in bilayer membranes, Chem. Phys. Lett. 298 (1998) 359–367.
[29] M.M.G. Krishna, N. Periasamy, Spectrally constrained global analysis of fluorescence decays in biomembrane systems, Anal. Biochem. 253 (1997) 1–7.
[30] G. Krishnamoorthy, Temperature jump as a new technique

to study the kinetics of fast transport of protons across membranes, Biochemistry 25 (1986) 6666–6671.
[31] N. Periasamy, S. Doraiswamy, B.G. Maiya, B. Venkataraman, Diffusion controlled reactions: fluorescence quenching of cationic dyes by charged quenchers, J. Chem. Phys. 88 (1988) 1638–1651.
[32] K.V. Bankar, V.R. Bhagat, R. Das, S. Doraiswamy, A.S. Ghangrekar, D.S. Kamat, N. Periasamy, V.J.P. Srivatsovoy, B. Venkataraman, Techniques for the study of fast chemical processes with half-times of the order of microseconds or less, Indian J. Pure Appl. Chem. 27 (1989) 416–428.
[33] A. Grinvald, I.Z. Steinberg, On the analysis of fluorescence decay kinetics by the method of least-squares, Anal. Biochem. 59 (1974) 583–598.
[34] P.R. Bevington, D.K. Robinson, Data Reduction and Error Analysis for the Physical Sciences, 2nd edn., McGraw-Hill, New York, 1994.
[35] J.R. Knutson, J.M. Beechem, L. Brand, Simultaneous analysis of multiple fluorescence decay curves: a global approach, Chem. Phys. Lett. 102 (1983) 501–507.
[36] D. Toptygin, J. Svobodova, I. Konopasek, L. Brand, Fluorescence decay and depolarization in membranes, J. Chem. Phys. 96 (1992) 7919–7930.
[37] B.A. Lewis, D.M. Engelman, Lipid bilayer thickness varies linearly with acyl chain length in fluid phosphatidylcholine vesicles, J. Mol. Biol. 166 (1983) 211–217.
[38] M.K. Jain, R.C. Wagner, Introduction to Biological Membranes, John Wiley and Sons, New York, 1980.
[39] C.G. Knight (Ed.), Liposomes: from Physical Structure to Therapeutic Applications, Elsevier, Amsterdam, 1981.
[40] M.P. Heyn, Determination of lipid order parameters and rotational correlation times from fluorescence depolarization experiments, FEBS Lett. 108 (1979) 359–364.
[41] F. Jahnig, Structural order of lipids and proteins in membranes: evaluation of fluorescence anisotropy data, Proc. Natl. Acad. Sci. USA 76 (1979) 6361–6365.
[42] D.P. Tieleman, S.J. Marrink, H.J.C. Berendsen, A computer perspective of membranes: molecular dynamics studies of lipid bilayer systems, Biochim. Biophys. Acta 1331 (1997) 235–270.
[43] C. Tanford, The Hydrophobic Effect: Formation of Micelles and Biological Membranes, 2nd edn., John Wiley and Sons, New York, 1980.
[44] P. Huang, J.J. Perez, G.H. Loew, Molecular dynamics simulations of phospholipid bilayers, J. Biomol. Struct. Dyn. 11 (1994) 927–956.
[45] H. Heller, M. Schaefer, K. Schulten, Molecular dynamics simulation of a bilayer of 200 lipids in the gel and in the liquid-crystal phases, J. Phys. Chem. 97 (1993) 8343–8360.
[46] G.L. Jendrasiak, J.H. Hasty, The hydration of phospholipids, Biochim. Biophys. Acta 337 (1974) 79–91.
[47] Y.K. Levine, N.J.M. Birdsall, A.G. Lee, J.C. Metcalfe, ^{13}C Nuclear magnetic resonance relaxation measurements of synthetic lecithins and the effect of spin-labeled lipids, Biochemistry 11 (1972) 1416–1421.